Bimodal control of three-dimensional wakes

Philippe Poncet

Bimodal control of three-dimensional wakes

Philippe Poncet

Laboratoire MIP, Dept GMM, INSA Toulouse,
135 avenue de Rangueil, 31077 Toulouse Cedex 4
Philippe.Poncet@insa-toulouse.fr

Summary. This paper investigates control strategies for drag reduction of three-dimensional wake generated by a circular cylinder at Reynolds number $Re = 300$, such flows presenting mode B instabilities whose main feature is streamwise finger-shaped eddies. The control is performed thanks to a field of tangential velocities on the cylinder. One first focuses on two-dimensional velocity fiels (spanwise invariant), using both a clustering genetic algorithm (see [7]) and Newton algorithm in Fourier space with five Fourier modes. Besically the same field comes out, whatever the control technique used. A square-root regression of the drag reduction versus amplitude of the control leads to the formulation of an efficiency criterion. One then considers a class of spanwise harmonic perturbation of this quasi-optimal profile, leading to a two paramater optimization problem, involving amplitude and wavelength of the perturbation. A cartography of the efficiency with respect to these two parameters is finally obtained, showing regions of interest.

1 Methodology

One considers the full three-dimensional Navier-Stokes equations in their velocity-vorticity $(\mathbf{u}, \boldsymbol{\omega})$ formulation and in the context of external flows :

$$\frac{\partial \boldsymbol{\omega}}{\partial t} + \mathbf{u} \cdot \nabla \boldsymbol{\omega} - \boldsymbol{\omega} \cdot \nabla \mathbf{u} - \nu \Delta \boldsymbol{\omega} = 0 \tag{1}$$

with $\nabla \cdot \mathbf{u} = 0$ and $\nabla \times \mathbf{u} = \boldsymbol{\omega}$ in the domain, and $\mathbf{u} = 0$ on boundaries, ν being the kinematic viscosity and the velocity $\mathbf{u}$ satisfying far field condition

$$\lim_{|\mathbf{x}| \to \infty} \mathbf{u}(\mathbf{x}) = U_\infty \mathbf{e}_x$$

with $\mathbf{e}_x$ being the streamwise basis vector.

The numerical scheme used is an hybrid vortex in cell method, fully described in [5, 3], performing direct numerical simulation of equation (1). As a summary, a time splitting algorithm is used in order to split apart convective and diffusive effects. The diffusive part is solved using a large finite-difference stencil based on particle strength exchange methods, and the Chorin algorithm in the context of cylindrical geometry is used for kinematic boundary conditions.

The remaining convective part is exactly the Euler equations satisfying incompressibility and with only no-flow-through boundary condition $\mathbf{u} \cdot \mathbf{n} = 0$, where $\mathbf{n}$ is the inward normal field to body. It is solved using a Lagrangian method involving particles of vorticity-location-volume $(\boldsymbol{\omega}_i, \mathbf{x}_i, v_i)$, changing the Euler equation into a classical dynamical system :

$$\frac{\mathrm{d}\boldsymbol{\omega}_i}{\mathrm{d}t} = (\boldsymbol{\omega} \cdot \nabla \mathbf{u})_{\mathbf{x}=\mathbf{x}_i} \ , \quad \frac{\mathrm{d}\mathbf{x}_i}{\mathrm{d}t} = \mathbf{u}(\mathbf{x}_i) \ , \quad \frac{\mathrm{d}v_i}{\mathrm{d}t} = v_i \nabla \cdot \mathbf{u}(\mathbf{x}_i) = 0 \tag{2}$$

the velocity field being built by differentiation of stream, that is to say by solving Poisson equations on a grid, with back and forth interpolations between particles and grid (cf. [5]). In order to avoid holes or accumulation of particles, which is sometimes reported as a drawback of Lagrangian methods, frequent high order remeshing onto a uniform lattice is performed.

The Lagrangian formulation makes transport terms $\mathbf{u} \cdot \nabla \boldsymbol{\omega}$ in the Euler equations vanish from the dynamical system (2). The transport stability condition, which is extremely restrictive in practice, disappears as well and allows to use time steps hundred times larger than conventional methods, without significant lack of accuracy. This is especially interesting to reach large time scales and perform control beyond transient regimes.

This numerical scheme has been validated in many contexts, for examples : up to $Re = 9500$ for 2D wakes in complex geometries [4], and up to $Re = 1400$ in 3D with the dynamic of an oblique ring interacting with a flat body, from [3] and represented on figure 1. Three-dimensional wakes have been especially investigated in [8, 9] up to $Re = 1000$.

The understanding of the physics of wakes behind circular cylinders has considerably evolved during the last fifteen years, and is mainly governed by the Reynolds number $Re = U_\infty D/\nu$, D being the cylinder diameter. The transition from steady to periodic flow occuring around $Re = 47$ is a very well-known feature of wakes. The transition from 2D to 3D, breaking the spanwise invariance feature by means of two modes of instabilities, has been intensively tracked during the mid-nineties, numerically (see [12]), by Floquet analysis (see [1]) and experimentally (see [13]).

Around $Re = 190$, the wake turns spontaneously three-dimensional in large wavelength (close to four diameters) called mode A instability. Above $Re = 260$ the large 3D structures do not appear anymore and are replaced by finger-shaped instabilities of shorter wavelength (less than a diameter) called mode B. This kind of instabilities is the dominant feature up to $Re = 2000$, superposing with turbulence as inertial range grows, and is responsible of a drop of 25% of the drag coefficient.

In the present work, one considers cylinder wakes presenting mode B instabilities at $Re = 300$, whose vorticity is plotted on figure 2. The drag coefficient is computed over a large interval of time, plotted on figure 3, showing the high stability of the numerical scheme presented above.

Control of such wakes is performed by means of tangential field of velocity on body in the azimuth direction, that is to say vector $\mathbf{e}_\theta$ in standard cylindrical coordinates. This field of velocity is usually called profile.

Section 2 describes how an optimal profile for two-dimensional flows has been built and how it affects three-dimensional flows. Since drag decreases as energy of control increases, the drag reduction cannot be used as cost function for minimization, and an efficiency criterion is defined also in section 2.

Spanwise modulation of this profile is then introduced in section 3. Preliminary computations from [6] of short duration, thus having possibly transient effects, and involving only low mode numbers, have shown that drag reduction tends to be larger as mode number increases. Section 4 investigates this phenomenon with long runs and accurate statistics, showing that efficiency increases up to mode 3 and the decreases, independently of energy level.

2 Two-dimensional control of 3D wakes

One considers a control by means of a field of velocity tangential to body, here a circular cylinder. The piecewise constant formulation of such fields is usually called "belt actuators". Applying velocity $\mathbf{u}$ to the body surface involves a non-dimensional kinetic energy defined by

$$E_c^*(\mathbf{u}) = \frac{1}{2\,U_\infty^2 \sigma(\partial\Omega)} \int_{\partial\Omega} \mathbf{u}(\mathbf{x})^2 \,\mathrm{d}s \tag{3}$$

where $\sigma(\partial\Omega)$ is a measure of the body : $\sigma(\partial\Omega) = L\pi D$ is the body surface in 3D, L being the cylinder width, and $\sigma(\partial\Omega) = \pi D$ in 2D.

Concerning two-dimensional flows, an optimal profile of piecewise constant tangential velocities has been carried out in [7], using an energy-improved genetic algorithm operating over 16 panels, called clustering genetic algorithm (CGA). Such profiles being not continuous, whether considering the best or the most probable element of the population, one has symmetrized and smoothed this profile, using a composite sinus-rational regression (see [10] for example), obtaining the function $\mathbf{V_c}(\theta)$ plotted on figure 4.

As often for genetic algorithms, global optimality is questionable. In order to validate the profile obtained by smoothing the CGA profile, and show that it is not dependent on the numerical method or its parameters,

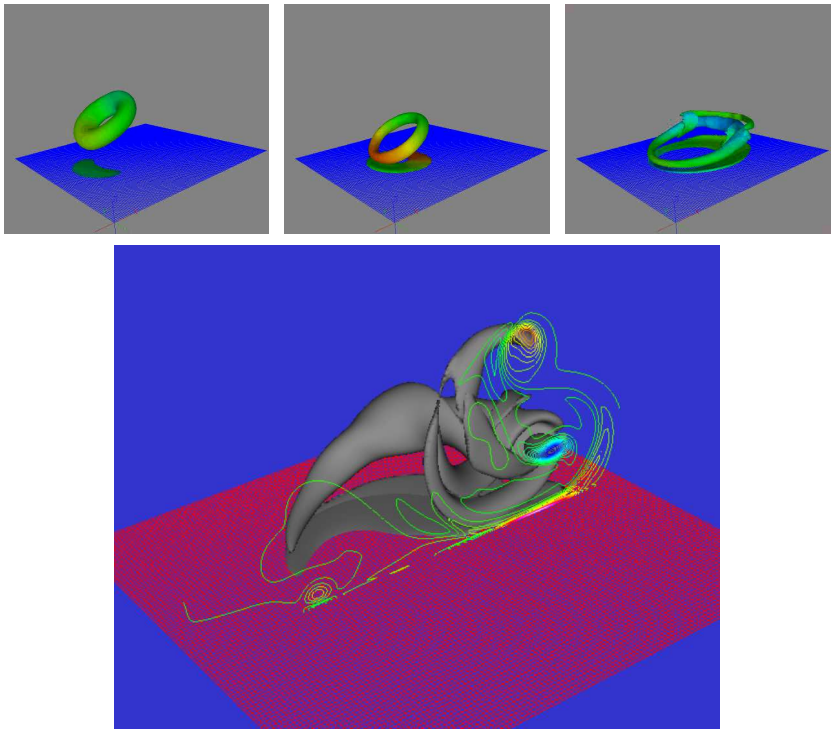

Fig. 1. Oblique annular vortex impinging into a wall at $Re = 1400$ (*Courtesy of G.H. Cottet*).

one has provided an other optimal control : the profile, function of angle, is searched as a combination of five Fourier modes and the minimization is performed by a Newton algorithm, involving 31 parallel runs for each step of minimization (1 central run, 5 for the gradient and 25 for the Hessian matrix). At the same energy level as the CGA, one finds a very strong similarity between profiles, for both maximal value and shape, plotted on figure 5.

In order to investigate control of three-dimensional wakes, one first considers a 3D flow controlled by this 2D profile with various amplitudes, that is to say $C\,\mathsf{V_c}(\theta)$ corresponding to an non-dimensional energy $C^2 E_c^*(\mathbf{V_c})$. Figure 6 shows plots of drag coefficients with respect to time for different values of amplitude C from 0.1 up to 2.0, and as qualitatively expected the drag reduction increases as the energy involved in the control increases. It has been shown in [6] that if energy is sufficiently high, the flow comes back to its nominal two-dimensional state.

Figure 6 also shows the mean post-transient drag reduction with respect to the amplitude C, and exhibits a square-root regression, discussed in [11]. This means that an efficiency criterion can be introduced :

$$Eff = (C_D^0 - C_D)/\sqrt{E_c^*} \tag{4}$$

where $C_D^0 = 1.374$ is the uncontrolled two-dimensional drag coefficient at $Re = 300$ for the present computations. As a consequence, the efficiency depends only on profile shape and not on the energy level for this 2D profile, thus provides a suitable cost function for three-dimensional control.

3 Bimodal control of 3D wakes

In order to introduce three-dimensionality in the control, one adds a spanwise harmonic perturbation to the optimal 2D profile, with a rescaling in order to conserve energy. Vector orientation is kept azimuthal, that is to say parallel to basis vector $\mathbf{e}_\theta$ in usual cylindrical coordinates. In order to reduce control space dimension, as a first approach, one also considers a profile with stagnation points and without local reverse velocity. This leads to the function

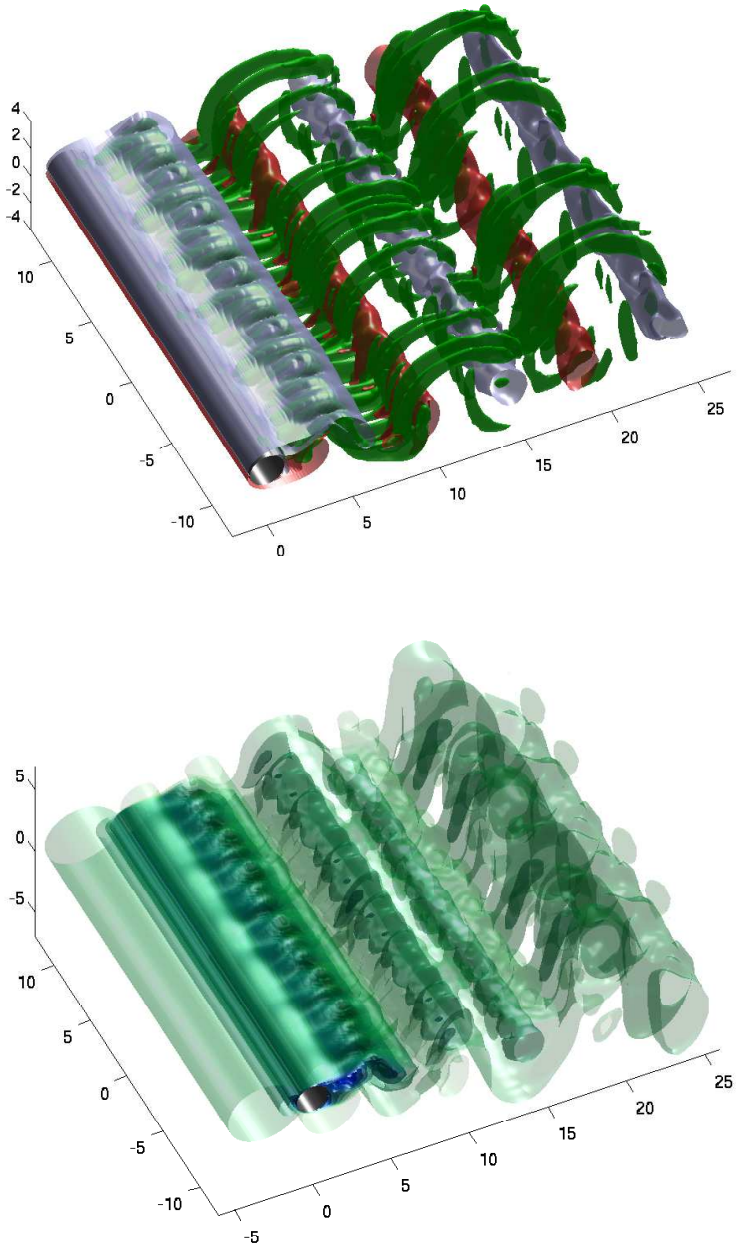

Fig. 2. Vorticity (to the top) and streamwise velocity (to the bottom) isovalues of uncontrolled flow at Reynolds number $Re = 300$.

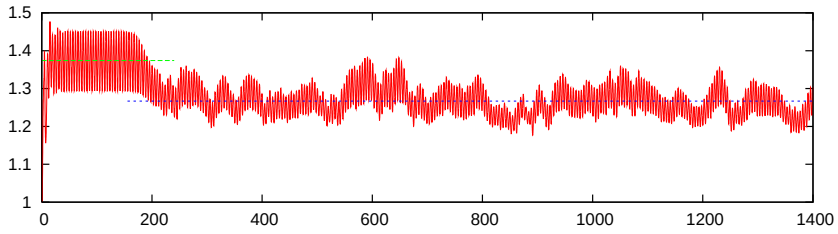

Fig. 3. Drag coefficient of a 3D wake at $Re = 300$. Early stage is periodic, until instabilities become dominant, leading to more chaotic values.

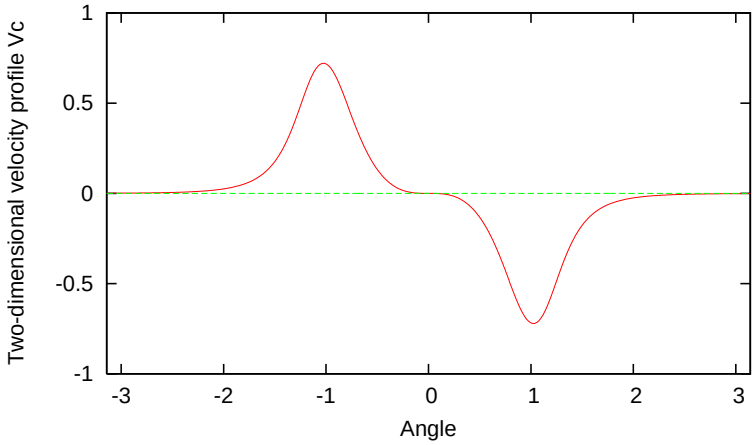

Fig. 4. Function $\mathbf{V_c}(\theta)$ used for 2D control, obtained by smoothing profile from Clustering Genetic Algorithm.

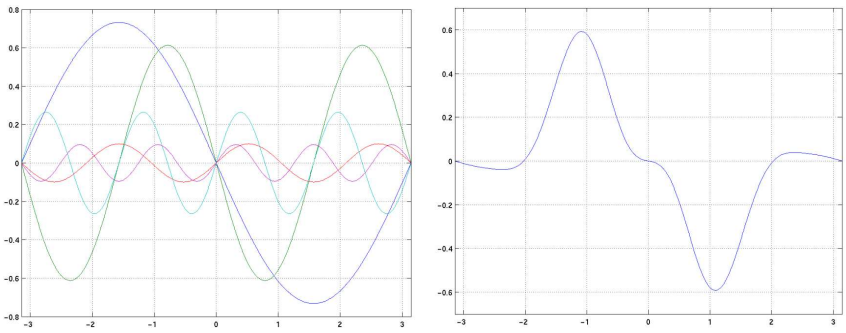

Fig. 5. Optimal modes (left picture) and 2D profile (right picture) for control of 3D flow using a Newton algorithm with five Fourier modes (*Courtesy of Roland Hildebrand*).

$$\mathbf{u}(\theta, z) = C\sqrt{2/3}\,(1 + \sin(kz))\,\mathbf{V_c}(\theta) \tag{5}$$

which depends on integer mode k and real amplitude C. Such a profile involves constant mode and mode of number k (being consequently a bimodal control). This three-dimensional profile is at the same level of energy as 2D profile, that is to say $C^2 E_c^*(\mathbf{V_c})$. Typical flow obtained with such a control is represented on figure 7, here for $k = 4$ and $C = 1.0$.

After having checked that the final drag does not depend on control activation time, one has computed efficiencies for $k = 1..8$ and from $C = 0.1$ up to $C = 1.1$.In order to exhibit the couple mode/amplitude of highest efficiency, a diagram of isoefficiency is plotted on figure 8.

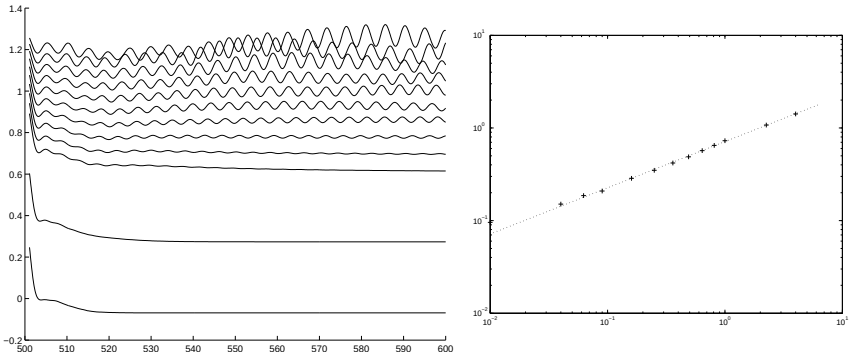

Fig. 6. Drag versus time for several values of amplitude C (to the left) and mean drag versus C (to the right) with square-root regression.

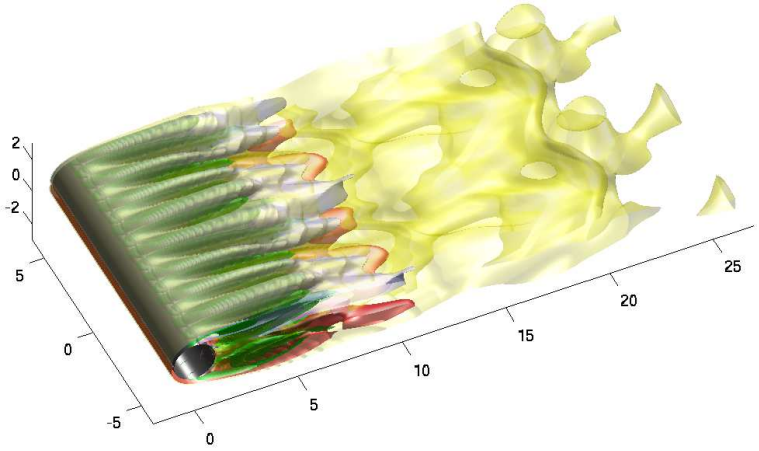

Fig. 7. Isovorticity surface of flow for mode $k = 4$ and $C = 1$. Levels at $\omega_z = \pm 0.7$, $\omega^{\perp} = 0.7$ and $|\boldsymbol{\omega}| = 0.3$.

According to this $C - k$ cartography, the maximum efficiency is found to be for modes 2 and 3, with amplitude around 0.65. The first noticeable fact is that nothing significant occurs at mode $k = 4$ which is the main growth mode of instability (mode B) at this Reynolds number. Indeed, a stronger interaction between natural instabilities and a control at the same wavelength could have been expected.

Moreover, signification of local extrema at low energy is questionable due to the lack of periodicity of the drag coefficient signal for the uncontrolled flow, thus for low amplitude controlled flow (at larger energies signal is periodic). The only significant low-energy minimum occurs at $k = 1$ and $C = 0.22$: this reduces speed difference between body and far field, and consequently reduces strain, which locally comes to consider a flow at $Re = 220$. At such a Reynolds number, instability of mode A is the main mode of instability, creating large structures (see figure 9) and influencing dramatically the drag coefficient [2]. Note that this control does not interact with mode A, but allows it to exist by generating the right window of strain value.

To the opposite, high mode control fields (k above 6) lead to non-optimal stable states for which the flows are strongly separated (see figure 10). Furthermore, for amplitudes above $C = 0.76$, zones of larger velocities than far field appear on body, and consequently physics of wakes is replaced by physics of jets as energy increases. Such a modification of the physics is probably responsible for the lack of efficiency at high energy.

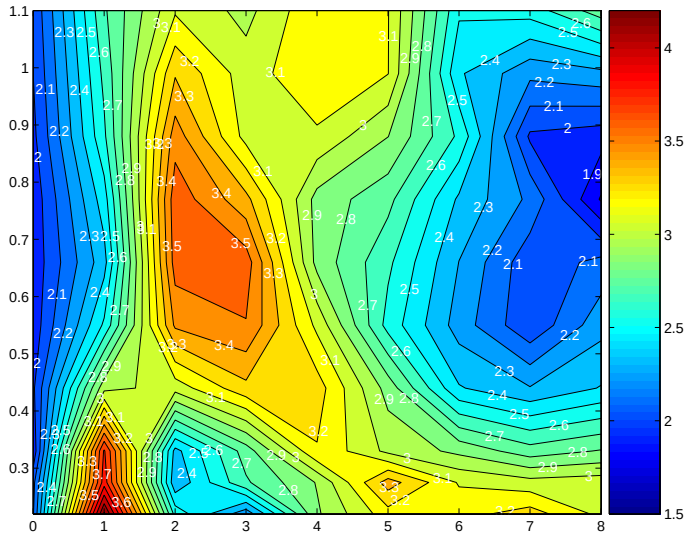

Fig. 8. Isolines of efficiency with respect to mode k and amplitude C.

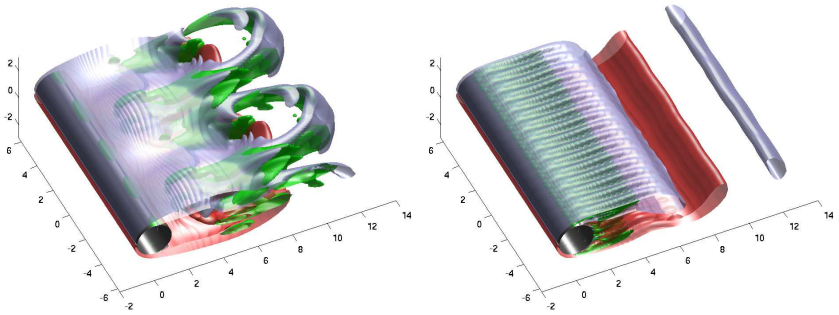

Fig. 9. Vorticity field at low mode and low energy with apparently stable mode A instability ($k = 1, C = 0.3$, to the left), and at high mode and high energy ($k = 8, C = 1.1$, to the right).

4 Conclusion

A highly stable numerical method has been used for three-dimensional direct numerical simulation of the wake behind a circular cylinder. The problem of control of drag coefficient has then been investigated, considering velocity profiles tangential to body.

An efficiency criterion been defined, and used for optimization since the drag reduction has been shown to be not suitable as a cost function. Optimal two-dimensional profile has been put forward for 2D and 3D flows.

An harmonic perturbation of this profile has then been used to perform control of 3D wakes, and the impact of this perturbation wavelength is discussed. It appears that efficiency increases as wavelength decreases down to wave number 3, that is to say about one diameter, with an optimal amplitude $C = 0.65$. Smaller wavelengths make efficiency decrease.

The question of optimal profiles with different combination between constant mode and harmonic perturbation, or multi-modal optimization is left open, work being under progress.

The author would like to thank Georges-Henri Cottet, Petros Koumoutsakos, Roland Hildebrand and Michele Milano for their invaluable help in the elaboration of this work. The computational resources have been provided by CalMiP (CICT, Toulouse, France), LMC (Grenoble, France) and INSA (Toulouse, France).

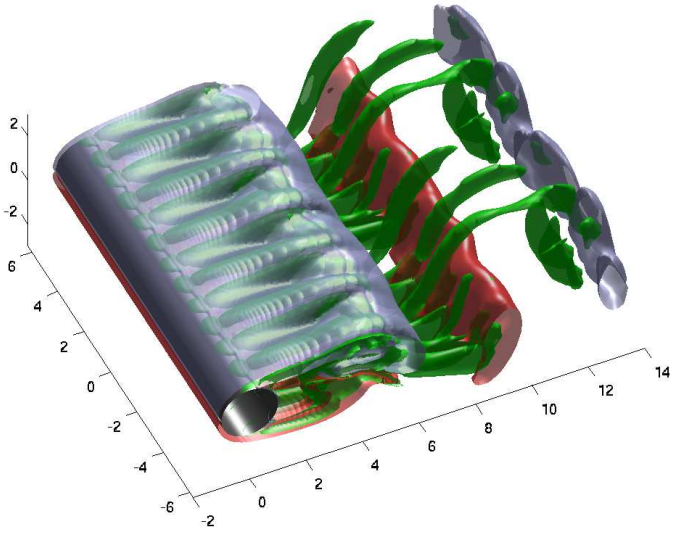

Fig. 10. Vorticity field in the optimal region ($k = 3, C = 0.6$).

References

1. Barkley D, Henderson R D (1996) J. Fluid Mech. 332:215–241
2. Blackburn H M, Henderson R D (1999) J. Fluid Mech. 385:255-286
3. Cottet G-H, Koumoutsakos P (2000) Vortex Methods, Theory and Practice. Cambridge University Press
4. Cottet G-H, Poncet P (2002) J. Turbulence 3(038):1–9
5. Cottet G-H, Poncet P (2003) J. Comp. Phys. 193:136–158
6. Cottet G-H, Poncet P (2004) Comput. Fluids 33:687–713
7. Milano M, Koumoutakos P (2002) J. Comp. Phys. 175:79-107
8. Poncet P (2002) Phys. Fluids 14(6):2021–2024
9. Poncet P (2004) J. Fluid Mech. 517:27–53
10. Poncet P, Koumoutsakos P (2005) Intl. J. Offshore Polar Eng. 15(1):1–7
11. Poncet P, Cottet G-H, Koumoutsakos P (2005) CR Mecanique 333:65–77
12. Thompson M, Hourigan K, Sheridan J (1996) Exp. Therm. Fluid Sci. 12:190–196
13. C.H.K. Williamson (1996) J. Fluid Mech. 328:345–407